JST: Engineering and Technology for Sustainable Development
Volume 33, Issue 2, April 2023, 044-051

First-Principles Study of Electronic and Optical Properties and Photocatalytic Performance of MS Monolayer under Strain

Nguyen Hoang Linh[1], Tran The Quang[2], Nguyen Minh Son[1], Nguyen Van Hoi[3], Vuong Van Thanh[1], Do Van Truong[1*]
[1]Hanoi University of Science and Technology, Ha Noi, Vietnam
[2] Thai Binh University, Thai Binh, Vietnam
[3]Jeonbuk National University, Republic of Korea
[*]Corresponding author email: truong.dovan@hust.edu.vn

Abstract

The study explores the mechanical, optoelectrical and photocatalytic properties of GeS and SnS structures by Density Function Theory (DFT) through Quantum Espresso software. The results show that the GeS and SnS structures are the semiconductor materials at equilibrium with band gaps of 1.75 eV and 1.4 eV, respectively. The band gap of these two structures tends to increase under the tensile strain and decrease under the compressive strain. Especially, at the strain of -10%, the band gap of GeS decreases dramatically and becomes metallic, while the SnS still maintains the semiconductor properties. The absorption coefficient is changed significantly in the ultraviolet region under the biaxial strain. Besides, our calculations also show that the GeS and SnS have photocatalytic properties and can become good candidates for overall water-splitting under the tensile strain. The results obtained from this study are the basis for application in microelectromechanical and optoelectronic devices and cleaning technology.

Keywords: 2D materials, DFT calculations, energy band structure, optical property, photocatalytic.

1. Introduction

After the advent of graphene [1], the studied properties of nanostructured materials have become an urgent topic [2, 3]. Compared to the traditional bulk material, 2D structures have great application potential and novel properties, which are brilliant candidates for electronic and optoelectronic devices. There are more than 100 elements of 2D structures have been discovered and studied in theory and experiments such as monochalcogenides, transition metal dichalcogenides (TMDs), Black phosphorus, Janus monolayers, pentagonal monolayers [4, 5].

Recently, monolayer structures such as GeS and SnS have been attracting lots of attention because their optical and electronic properties can be applied in optoelectronic devices, sensors and energy storage, water split technology, photodetectors and solar cells [6]. Liu *et al*. have demonstrated that two structures GeS and SnS are successfully synthesized in the laboratory, they have semiconductor properties and can be applied to highly efficient photodetectors [7]. Tan *et al.* have shown that the SnS structure is a promising thermoelectric material with low thermal conductivity and a high Seebeck coefficient. In addition, this study has also indicated that thermoelectric efficiency is enhanced through the ZT coefficient by the Ag atom doping method [8].

As we all know, in some structures, the strain appears undesirable and causes some changes in the properties of a material. The effect of strain on the electronic and optical properties has been demonstrated by Khang [9], Fatahin [10]. Recently, based on the change of material properties under the strain, many studies have focused on determining the reasonable strain regions to improve the electronic, optical and photocatalytic properties [11] of material. In this study, the effect of the biaxial strain on the electronic, optical and photocatalytic properties of two SnS and GeS structures is evaluated through first-principle calculations. The obtained results show that the strain significantly affects the band gap and the light absorption coefficient of the two structures. The photocatalytic properties appear under the tensile strain in the SnS structure and are suppressed in the GeS structure. Moreover, mechanical properties such as the elastic modulus and Poisson's ratio of two materials are explored as well.

2. Methodology

The ab-initio calculation method based on density functional theory DFT through Quantum Espresso software was used to simulate and investigated the properties of materials. Electron interactions were described by Vanderbilt pseudopotentials (USSP) with exchange-correlation

ISSN 2734-9381
https://doi.org/10.51316/jst.165.etsd.2023.33.2.7
Received: October 10, 2022; accepted: February 10, 2023

energy determined by the generalized gradient approximation (GGA) through Perdew-Burke-Ernzerhof (PBE) functional. The cutoff energy and charge density for plane wave functional were taken by 60 Ry and 720 Ry, respectively. The *k*-grid in the Brillouin zone was taken as 17×17×1 through the Monkhorst-Pack method.

Fig. 1 illustrates the structure of the MS monolayer (M: Ge, Sn). Durcalculationting, the periodic boundary conditions were applied in all three directions. A vacuum space was set in the *z* direction with a thickness of 30 Å to avoid interactions between the layers [12]. The crystal parameters of MS structures were explored through the Broyden-Fletcher-Goldfarb-Shanno (BFGS) algorithm with the stress and force conditions less than 5.10^{-2} GPa and 10^{-6} Ry/a.u at 0K, respectively [13]. The mechanical strain on the monolayer structure was calculated by the following equation:

$$\varepsilon = \left(\frac{l_1}{l_0} - 1\right).100\% \quad (1)$$

where l_1, l_0 are the lattice parameters in the strain state ($\varepsilon \neq 0$) and the equilibrium state ($\varepsilon = 0$). In this study, we investigated the biaxial strain in the strain range ±10% as shown in Fig 1.

3. Results and Discussion

3.1. Mechanical Properties

After relaxing by the BFGS method, we obtain the relationship between the total energy and the lattice parameters as shown in Fig 2. The corresponding lattice vectors of GeS and SnS are a = 4.44 Å, b = 3.66 Å and a = 4.33 Å, b = 4.05 Å (at the red points in Fig. 2). These results are similar to that of the previous studies [14] and the experiments [15]. The mechanical properties of structures are described through the C_{ij} elastic constants calculated by using the Thermo-Pw code. The elastic module and Poisson's ratio are calculated from elastic constants according to following equation:

$$E_x = \frac{C_{11}.C_{22} - C_{12}^2}{C_{22}}; \quad E_y = \frac{C_{11}.C_{22} - C_{12}^2}{C_{11}} \quad (2)$$

$$\upsilon_x = \frac{C_{12}}{C_{22}}; \quad \upsilon_y = \frac{C_{12}}{C_{11}} \quad (3)$$

Our calculation results show that the SnS structure has an elastic modulus in both x and y directions of 10.47 N/m (E_x) and 23.93 N/m (E_y) respectively, smaller than the elastic modulus of GeS 11.61 N/m (E_x) – 27.40 N/m (E_y). Table 1 lists the results obtained as the lattice parameters a, b (Å), thickness h (Å), the elastic constant C_{ij} (N/m), the elastic modulus E (N/m) and the Poisson's ratio υ of two structures. In general, the MS material structures possess a rather small set of mechanical parameters compared to the previously studied 2D materials such as γ-GeS (E = 99.67 N/m) or γ-GeSe (E = 93.42 N/m) or γ-GeTe (E = 81.89 N/m) [13]. These results can confirm that the MS structures have quite flexible mechanical properties.

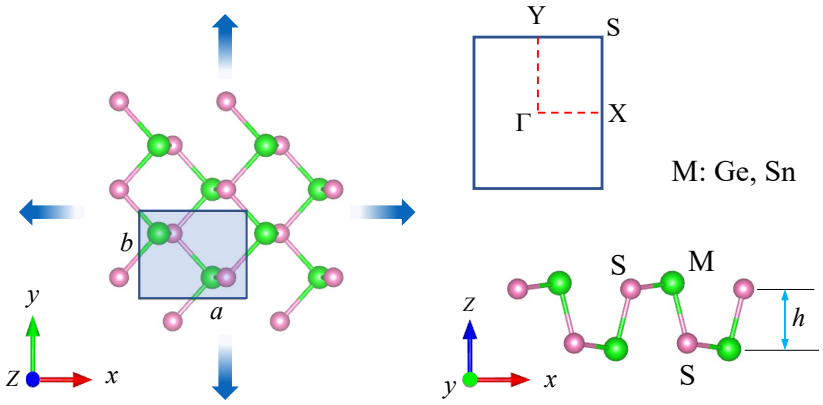

Fig. 1. The MS structures (M: Ge, Sn) and their reciprocal region with high symmetry points

Table 1. Lattice parameters a, b (Å), thickness h (Å), elastic constant C_{ij} (N/m), elastic modulus E (N/m) and Poisson's ratio υ.

Monolayer	a	b	h	C_{11}	C_{12}	C_{22}	C_{66}	E_x - E_y	υ_x - υ_y
GeS	4.44	3.66	2.36	19.12	18.4	45.1	16.81	11.61 – 27.40	0.408 – 0.96
SnS	4.33	4.05	2.58	17.26	16.37	39.46	16.21	10.47 – 23.93	0.410 – 0.948

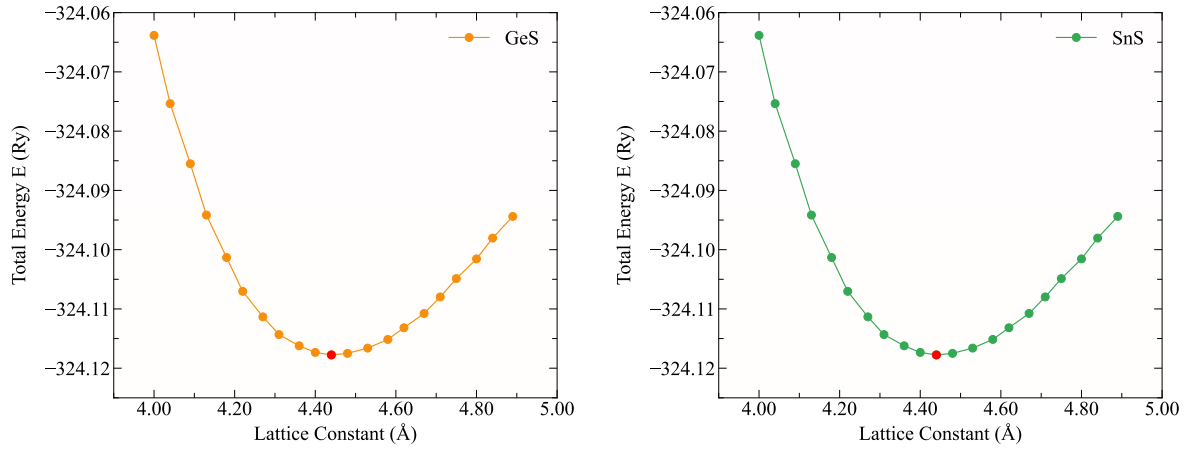

Fig. 2. The relationship between lattice constant and total energy system

3.2. Electronic Properties

To understand the change in the electronic properties of GeS and SnS under the strain, this study investigates the energy band structures of GeS and SnS at several strains as shown in Fig 3. The band gap is defined as the distance between the conduction-band minimum (CBM) and the valence-band maximum (VBM). Since the GeS and SnS structures are orthorhombic lattices and the Brillouin zone does not change under the strain, the Brillouin zone is taken in S-X-Γ-Y-S. At equilibrium (ε_{bia} = 0%), GeS and SnS exhibit the indirect semiconductor properties with a band gap of 1.75 eV and 1.4 eV, respectively. The results are also analogous to that of the previous study [9]. The CBM of GeS is located at the Γ-Y path, and the VBM is at the Γ point. Under the tensile strain, the CBM changes in the range from Γ-Y to Γ-X, while the VBM remains at the Γ point. Conversely, for the compressive strain, the VBM is moved from the Γ point to the X-Γ path and the CBM stays on at the Γ point. Interestingly, at the strain ε_{bia} = -10%, GeS becomes a metal material with a band gap of 0 eV. Turning to SnS which has the VBM and the CBM in the Γ-X and the Γ-X paths, respectively. Under the compressive strain, the CBM is transferred to the Γ point, while the VBM keeps the same position. On the other hand, the tensile strain changes the CBM range which is moved to the Γ-X range but does not change the position of the VBM point.

Fig. 4 exhibits the relationship between the band gap and the biaxial strain (ε_{bia}) in the range from -10% to 10%. The band gap of GeS and SnS demonstrated expands rapidly under the strain from 0% to 3% and reaches its peak at ε_{bia} = 3% with 1.92 eV for GeS and 1.76 eV for SnS. However, in the next stage, the band gap of GeS and SnS decreases slightly and converges to a value of 1.65 eV at ε_{bia} = 10%. In contrast, under the compressive strain, the band gap of GeS decreases dramatically and becomes metallic at the strain of -10%, while the band gap of SnS is changed, decreasing about 30% at the strain of -7% but increasing again to 1.11 eV at the strain of -10%. Thus, the SnS still maintains the semiconductor properties under the biaxial strain within ±10%. The semiconductor properties of the GeS disappeared at the strain of -10%. These obtained results can confirm that mechanical strain can control the electronic band structures and the band gap.

3.3. Photocatalytic Properties

Recently, the photocatalytic properties of monolayer materials have been widely applied in the cleaning industry [11]. Based on these properties, the monolayer materials can be used in hydrogen production via water splitting under solar radiation. This study investigates the photocatalytic properties of two structures GeS and SnS under the biaxial strain within ±10%.

$$E^{red}_{H^+/H_2} = pH \times 0.059 \quad eV, \tag{4}$$

$$E^{ox}_{O_2/H_2O} = 1.23 + pH \times 0.059 \quad eV \tag{5}$$

We use (4) and (5) to convert the pH of the reduction potential H^+/H_2O and the oxidation potential O_2/H_2O to the energy of the redox reaction. Material good for water splitting applications if the position of the CBM is above the reduction potential (0 eV), the position of the VBM is below the oxidation potential (1.23 eV), and the distance between the CBM and the VBM is higher than 1.23 eV compared the normal hydrogen electrode (NHE).

Fig. 5 illustrates the position of CBM and VBM edges for the GeS and SnS structures. We note that two dash lines are the reduction potential H^+/H_2O and the oxidation potential O_2/H_2O at pH = 0 according to NHE.

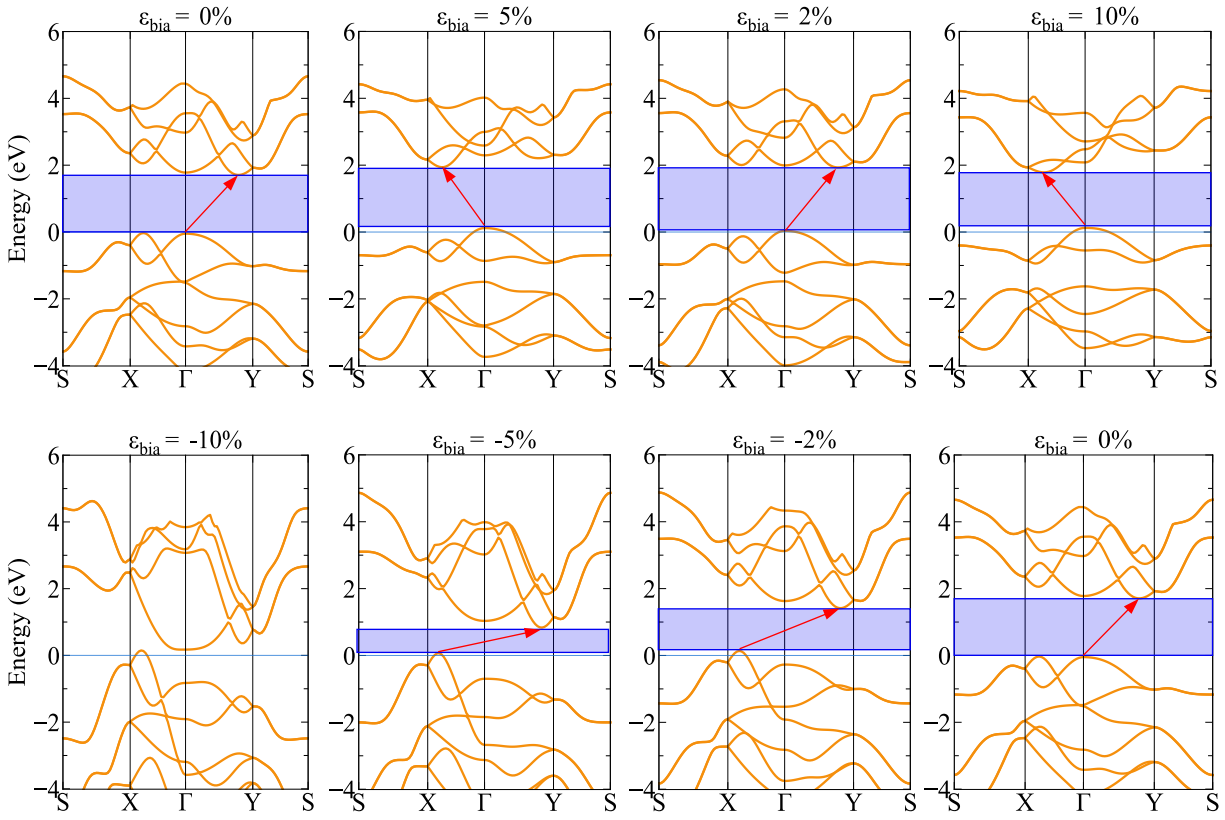

(a)

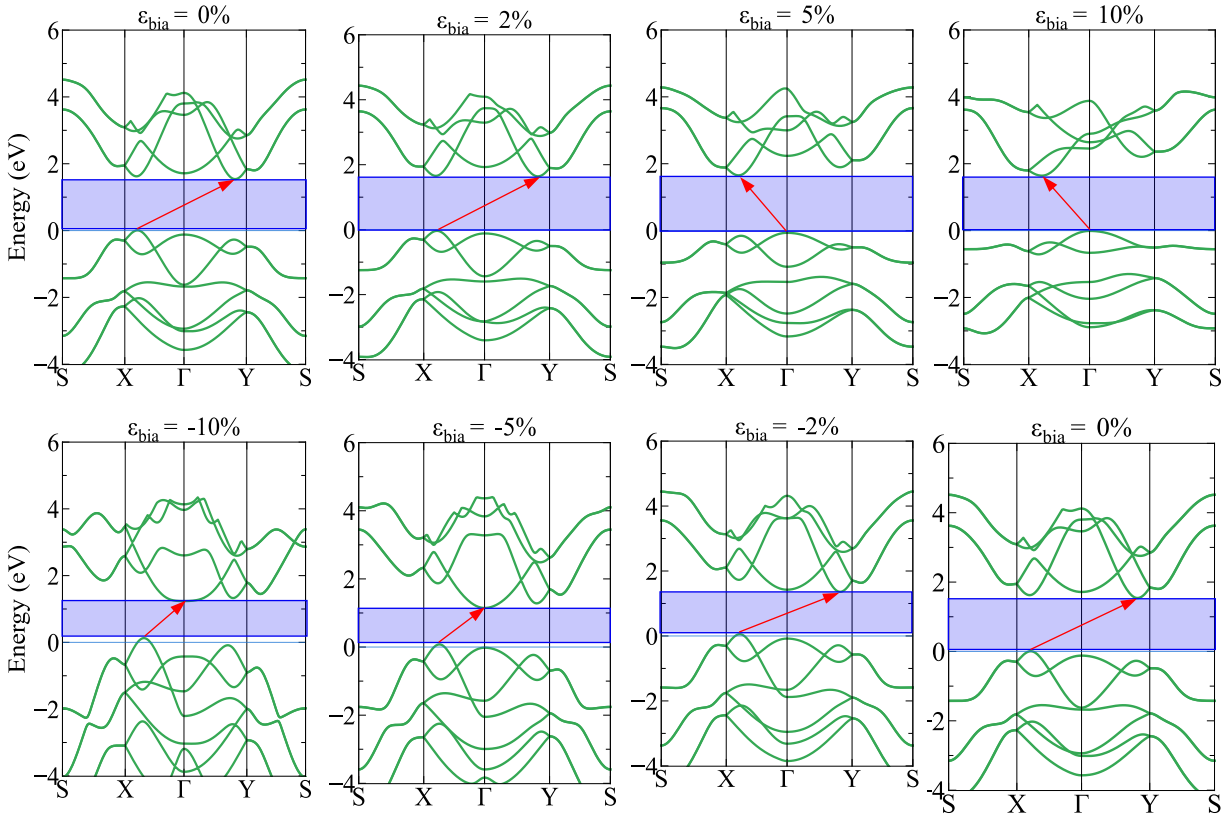

(b)

Fig. 3. Energy band structures of monolayer *(a)* GeS and *(b)* SnS under biaxial strains

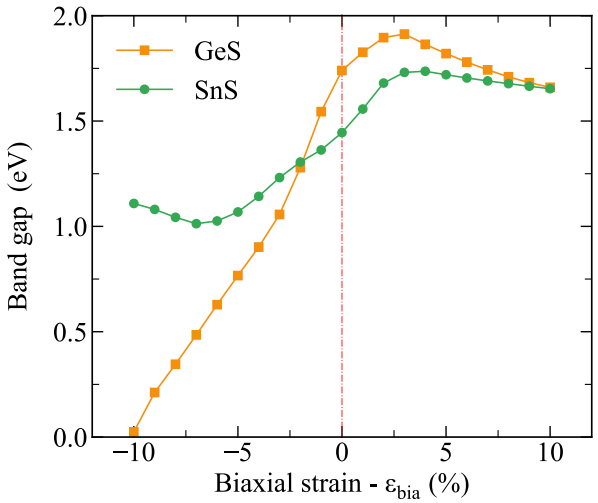

Fig. 4. Band gaps of MS monolayer as a function of biaxial strain ε_{bia}

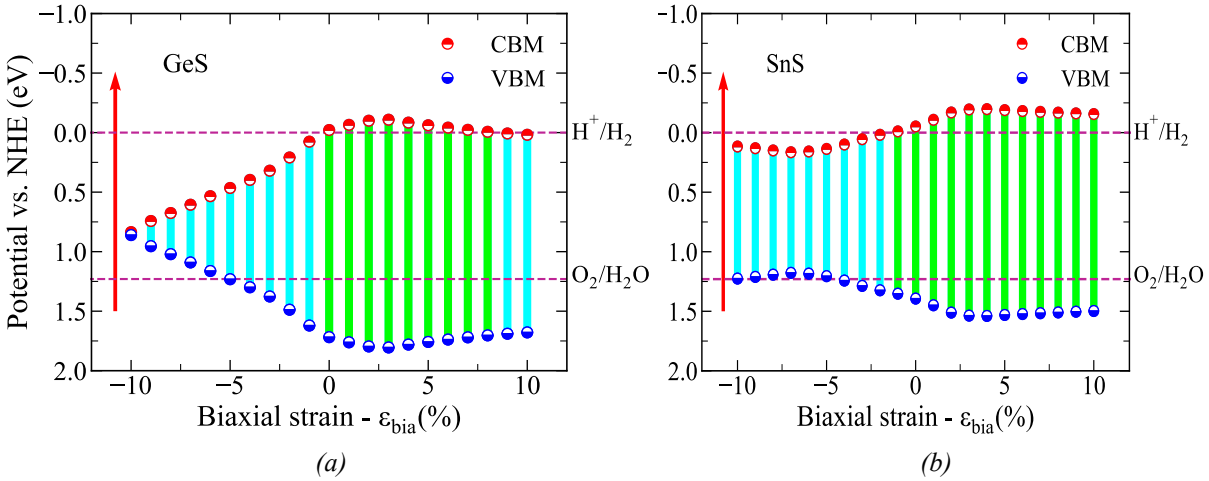

Fig. 5. Photocatalytic properties of GeS *(a)* and SnS *(b)* structures under biaxial strain

Our results show that the GeS and SnS structures have photocatalytic potential in their natural state. The CBM edge position of GeS and SnS structures are -0.02 eV and -0.05 eV, which is higher than the reduction potential H^+/H_2O. Contemporaneously, their VBM edge position with values of 1.72 eV and 1.39 eV, respectively, are lower than the oxidation potential. Under the tensile strain, the photocatalytic of two structures is enhanced when the position of CBM tends higher than the reduction potential, and VBM tends lower than the oxidation potential. However, the GeS structure lost the reduction at the strain $\varepsilon_{bia} > 8\%$ as the potential of CBM cannot satisfy the stated conditions, Fig. 5(a). Oppositely, the two structures fade the photocatalytic properties under the compressive strain because their band gaps decrease. The position of CBM and VBM does not satisfy the conditions for performing a redox reaction because two structures have the CBM edge always lower than the reduction potential, and the VBM edge always higher than the oxidation potential. Therefore, the GeS and SnS monolayers can perform the water splitting process under the tensile strain.

3.4. Optical Properties

In this section, the optical properties of the monolayer MS are explored with the PBE functional. The study calculates the light absorption coefficient according to the equation:

$$\alpha(\omega) = \frac{\sqrt{2}\omega}{c}\left(\sqrt{\varepsilon_1^2(\omega) + \varepsilon_2^2(\omega)} - \varepsilon_1(\omega)\right)^{1/2} \quad (6)$$

Here, α is the light absorption coefficient, $\varepsilon_1(\omega)$ is the real part calculated through the Kramer-Kronig transformation and $\varepsilon_2(\omega)$ is the imaginary part based on the sum of the occupied-unoccupied transitions. The effects of the biaxial strain on the light absorption coefficient α of GeS and SnS are shown in Fig. 6, 7.

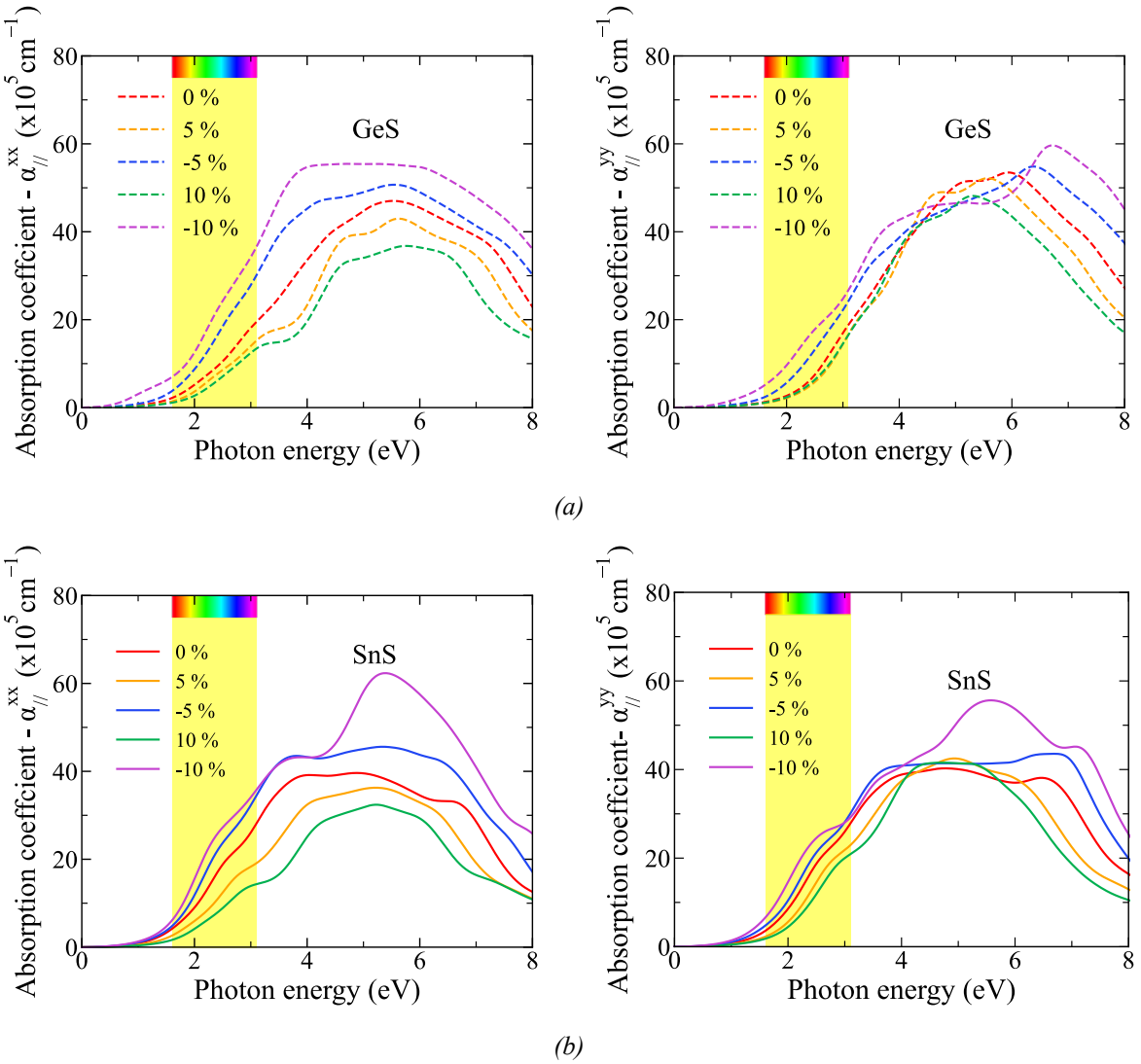

Fig. 6. Effect of the biaxial strain on the absorption coefficient of GeS *(a)* and SnS *(b)* structure in-plane direction

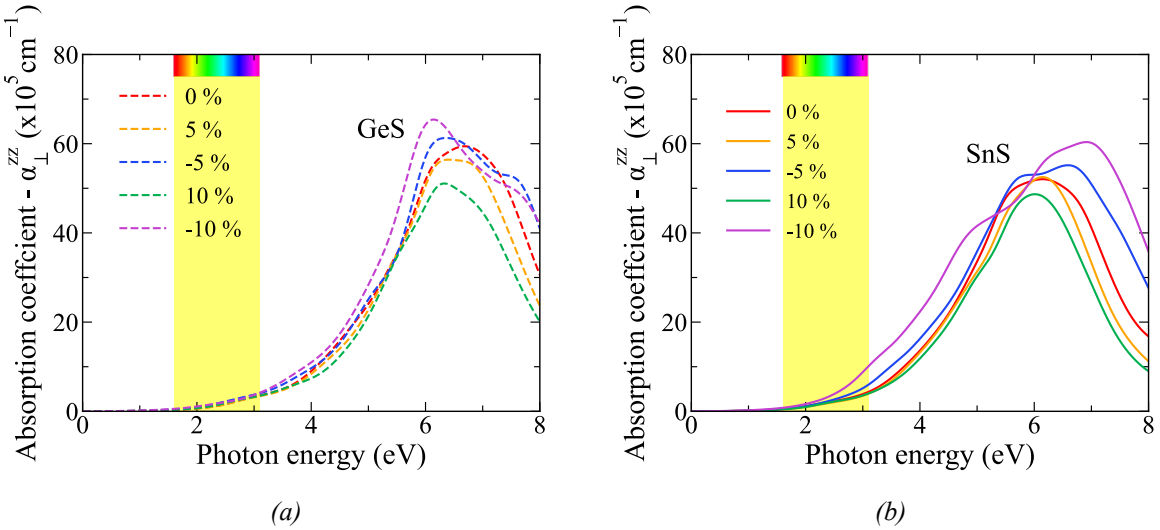

Fig. 7. Effect of the biaxial strain on the absorption coefficient of GeS *(a)* and SnS *(b)* structure out-of-plane direction

Generally, under the strain, the light absorption coefficients α of GeS and SnS tend to decrease under the tensile strain and increase under the compressive strain. The light absorption coefficients of GeS and SnS increase sharply under the photon energy in the range of visible light and a part of ultraviolet light. The light absorption coefficient tends to decrease gradually when reaching the saturation value.

For the in-plane direction, the light absorption coefficient of GeS in the *y* direction is greater than that in the *x* direction. In contrast, the light absorption coefficient of SnS has the opposite trend. Under the strain $\varepsilon_{bia} \neq 0\%$, the absorption coefficient gradually decreases in the *xy* plane, this decrease is evident in the *x* direction. At the compressive strain ε_{bia} = -10%, SnS and GeS have the saturation light absorption coefficients in the ultraviolet zone with the maximum values in the *x* and *y* directions, that are α_{xx} = 55.5 × 10^5 cm^{-1} (higher 18% than the equilibrium), α_{yy} = 59.6 × 10^5 cm^{-1} (higher 11.5%) for GeS, α_{xx} = 62.3 × 10^5 cm^{-1} (higher 57%), α_{yy} = 55.6 × 10^5 cm^{-1} (higher 38.7%) for SnS, Fig 6.

For the out-of-plane direction, the light absorption coefficient in the *z* direction is almost unchanged for the photon energies less than 6 eV. However, after reaching the saturation values at the photon energies within 6 eV to 8 eV, the light absorption coefficient α_{zz} decreases. At the strain ε_{bia} = -10%, the light absorption coefficient in the ultraviolet zone is the largest. Our calculations detect the maximum of the light absorption coefficients of GeS and SnS are α_{zz} = 65.4 × 10^5 cm^{-1} (higher 10% than the equilibrium state) and α_{zz} = 60.4 × 10^5 cm^{-1} (higher 16%), respectively, Fig. 7. The obtained results also show that the 2D structures GeS and SnS have the maximum light absorption coefficients higher than that in some materials such as the TMDs and Phosphorene group [8].

4. Conclusion

This research investigates the mechanical, electronic, optical and photocatalytic properties of the MS structures (M: Ge and Sn) through the first-principle method. The obtained results show that the GeS and SnS structures are the indirect semiconductor and the band gap of GeS and SnS can be changed under the strain. The light absorption coefficients α of GeS and SnS are larger than that of the previous TMDs such as MoS_2, WS_2 and Phosphorene, and are promising for applications in light-absorbing devices in the future. Both structures possess photocatalytic properties that are used in cleaning industries.

Reference

[1] K.S. Novoselov, A. K. Geim, S. V. Morozov, D. Jiang, Y. Zhang, S. V. Dubonos, I. V. Grigorieva, and A. A. Firsov, Electric field effect in atomically thin carbon films, Science, vol. 306, 666–669, 2004. https://doi.org/10.1126/science.1102896.

[2] D. Van Truong, T. T. Quang, N. H. Linh, N. Van Hoi, and V. Van Thanh, Strain effect on hysteresis loop of $PbTiO_3$ bulk, in Proceedings of the International Conference on Engineering Research and Applications, ICERA 2019, vol. 104, no. Springer, 2020, 679–685. https://doi.org/10.1007/978-3-030-37497-6_78.

[3] D. V. Truong, T. N. Giang, V. V. Thanh, and T. T. Quang, Deterministic control of toroidal moment in ferroelectric nanostructures by direct electrical field, Mater. Res. Bull., vol. 131, 110981, Nov. 2020. https://doi.org/10.1016/j.materresbull.2020.110981.

[4] Z. Guan *et al.*, Recent progress in two-dimensional ferroelectric materials, Adv. Electron. Mater., vol. 6, no. 1, 1–30, 2020. https://doi.org/10.1002/aelm.201900818.

[5] V. Van Thanh, D. Van Truong, and N. T. Hung, Charge-induced electromechanical actuation of two-dimensional hexagonal and pentagonal materials, Phys. Chem. Chem. Phys., vol. 21, no. 40, 22377–22384, 2019. https://doi.org/10.1039/c9cp03129d.

[6] C. Gong *et al.*, Electronic and optoelectronic applications based on 2D novel anisotropic transition metal dichalcogenides, Adv. Sci., vol. 4, no. 12, 2017. https://doi.org/10.1002/advs.201700231.

[7] P. Ramasamy, D. Kwak, D. H. Lim, H. S. Ra, and J. S. Lee, Solution synthesis of GeS and GeSe nanosheets for high-sensitivity photodetectors, J. Mater. Chem. C, vol. 4, no. 3, 479–485, 2016. https://doi.org/10.1039/c5tc03667d.

[8] L. C. Gomes, A. Carvalho, and A. H. Castro Neto, Vacancies and oxidation of two-dimensional group-IV monochalcogenides, Phys. Rev. B- Condens. Matter Mater. Phys., vol. 94, no. 5, 054103--10, 2016. https://doi.org/10.1103/PhysRevB.94.054103.

[9] K. D. Pham *et al.*, Ab-initio study of electronic and optical properties of biaxially deformed single-layer GeS, Superlattices Microstruct., vol. 120, 501–507, 2018. https://doi.org/10.1016/j.spmi.2018.06.013.

[10] N. Fatahi, D. M. Hoat, A. Laref, S. Amirian, A. H. Reshak, and M. Naseri, Erratum to: 2D Hexagonal SnTe monolayer: a quasi direct band gap semiconductor with strain sensitive electronic and optical properties, Eur. Phys. J. B, vol. 93, no. 7, 100543, 2020. https://doi.org/10.1140/epjb/e2020-10278-y.

[11] L. Tao and L. Huang, Computational design of enhanced photocatalytic activity of two-dimensional cadmium iodide, RSC Adv., vol. 7, no. 84, 53653–53657, 2017. https://doi.org/10.1039/c7ra09687a.

[12] V. Van Thanh, N. T. Hung, and D. Van Truong, Charge-induced electromechanical actuation of Mo- and W-dichalcogenide monolayers, RSC Adv., vol. 8, no. 67, 38667–38672, 2018. https://doi.org/10.1039/c8ra08248k.

[13] V. Van Thanh, N. D. Van, D. Van Truong, and N. T. Hung, Effects of strain and electric field on electronic and optical properties of monolayer γ-GeX (X = S, Se and Te), Appl. Surf. Sci., vol. 582, no. January, 2022. https://doi.org/10.1016/j.apsusc.2021.152321.

[14] R. Fei, W. Li, J. Li, and L. Yang, Giant piezoelectricity of monolayer group IV monochalcogenides: SnSe, SnS, GeSe, and GeS, Appl. Phys. Lett., vol. 107, no. 17, 173104–5, 2015. https://doi.org/10.1063/1.4934750.

[15] J. R. Brent *et al.*, Tin(II) Sulfide (SnS) nanosheets by liquid-phase exfoliation of herzenbergite: IV-VI main group two-dimensional atomic crystals, J. Am. Chem. Soc., vol. 137, no. 39, 12689–12696, Oct. 2015. https://doi.org/10.1021/jacs.5b08236.